J. Anat. (1984), **138**, 1, pp. 175–188
With 16 figures
Printed in Great Britian

Ultrastructural aspects of spermatogenesis in the common marmoset (*Callithrix jacchus*)

W. V. HOLT AND H. D. M. MOORE

Institute of Zoology, The Zoological Society of London, Regent's Park, London NW1 4RY

(*Accepted* 16 *June* 1983)

INTRODUCTION

The apparent paucity of morphological studies of spermatogenesis in New World monkeys, and indeed in subhuman primates as a group, contrasts with the growing use of these species as animal models for human reproduction. The main aim of the present study, therefore, is to provide a basic description of the spermatogenic cycle in the common marmoset, *Callithrix jacchus*, a New World monkey whose value as a laboratory animal is enhanced by its small body size, early age of sexual maturity and relatively high reproductive rate.

The duration of spermatogenesis and mode of spermatogonial renewal have been studied in some primates: *Macaca speciosa* (Antar, 1971); *Papio cynocephalus, Macaca mulatta, Cercopithecus sabaeus* and *Saimiri sciureus* (Barr, 1973); *Papio anubis* (Chowdhury & Steinberger, 1976); *Cercopithecus aethiops* (Clermont, 1969); *Macaca arctoides* (Clermont & Antar, 1973); *Macaca rhesus* (Clermont & Leblond, 1959), but few ultrastructural studies have been reported.

Some ultrastructural aspects of spermatogenesis have been described in the cotton-top tamarin *Sequinus oedipus* (Rattner & Brinkley, 1970), mainly concerning sperm tail formation, but the most comprehensive fine structural studies are reported in a series of publications dealing with the blood testis barrier, spermatogonia and with the later stages of spermatogenesis in *Macaca mulatta, M. arctoides* and *M. fascicularis* (Dym, 1973; Dym & Cavicchia, 1977, 1978; Cavicchia & Dym, 1978).

In the present report, a general ultrastructural account of spermatogenesis in the common marmoset is given. This is accompanied by a proposed system of classification of spermatogenic steps, which should prove useful not only as an aid to recognition of cell types in thin sections, but also for future studies which may involve toxicological, pharmacological or experimental treatments.

MATERIALS AND METHODS

Ten adult male common marmosets, *Callithrix jacchus*, were used in this study; testicular tissue was obtained from five animals anaesthetised by intramuscular injection of Saffan (Glaxovet Ltd) prior to vascular perfusion with 4% glutaraldehyde and 1% paraformaldehyde in 100 mM phosphate buffer (pH 7·4). Small pieces of testicular tissue from the other five animals were fixed by immersion. After fixation, the tissue samples were post-fixed in a mixture of 1% osmium tetroxide and 1·5% potassium ferrocyanide, dehydrated, embedded in Epon and sectioned for electron microscopy. Sections were stained with uranyl acetate and lead citrate (Venable & Coggeshall, 1965), and examined with an AEI EM6B electron microscope.

Some tissue samples were fixed in Bouin's or Helly's fluids for light microscopy, and subsequently embedded in paraffin wax. Sections 5 μm thick were stained using the iron haematoxylin/periodic acid–Schiff technique for the demonstration of acrosomal structures.

For high resolution light microscopy, the Epon-embedded tissues were sectioned at a thickness of 1 μm. Sections were either stained briefly with 1 % toluidine blue in 1 % borax at 60 °C, a particularly effective stain for the acrosome, or stained with a stabilised iron chloride haematoxylin (Lillie & Fullmer, 1976) for two hours, after prior removal of the epoxy resin with saturated ethanolic potassium hydroxide; this stain provided the fine nuclear detail essential for distinguishing the various stages of primary spermatocyte development.

Figure 1, showing the nine spermatogenic stages identified in the marmoset testes, was prepared with the aid of iron chloride haematoxylin-stained Epon sections. Appropriate cells were outlined in India ink on photographic prints which were subsequently bleached out to leave line drawings. The line drawings were used to assemble the diagram.

RESULTS

Light microscopy

The various generations of spermatogenic cells formed characteristic associations which occupied the whole region of seminiferous epithelium visible within any transverse section. Nine separate associations were consistently observed and were therefore defined as the nine individual stages of the normal spermatogenic cycle in the marmoset.

The nine stages are illustrated diagrammatically in Figure 1, and their main distinguishing features are outlined below.

The nine stages of spermatogenesis were associated with twelve steps in the development of the spermatid; the appearance of a new generation of spermatids (Step 1 spermatids) was used to define the first spermatogenic stage, in keeping with similar classifications developed for other species.

The cytological events immediately preceding the appearance of Step 1 spermatids, i.e. the production and subsequent division of secondary spermatocytes, therefore defined the ninth stage of spermatogenesis. The transient nature of the secondary spermatocytes led to the frequent observation of meiotic figures as a feature of Stage IX. To avoid an unnecessarily complex system of classification, the presence of such meiotic figures was not used to define additional spermatogenic stages.

Stages II and III of the spermatogenic cycle were distinguished mainly on the basis of spermatid morphology. The transition from Stage II to III involved the adhesion of the acrosomal vacuole to the nuclear membrane of the Step 2/3 spermatids, and the formation and subsequent release of the residual body in the older (Step 11/12) spermatid generation.

Fig. 1. Nine successive stages of spermatogenesis in the marmoset are shown in this drawing, which was prepared using haematoxylin-stained Epon sections. The columns of stages, labelled with Roman numerals, represent the cell associations found in individual areas of the seminiferous epithelium. Steps of spermatid development are numbered from 1 to 12.

The letters A_1, A_2 and B, refer to Type A dark, Type A light, and Type B spermatogonia, respectively. Steps of spermatocyte development, i.e. preleptotene, leptotene, zygotene, pachytene, and secondary spermatocytes are represented by the letters PL, L, Z, P and Sp II respectively.

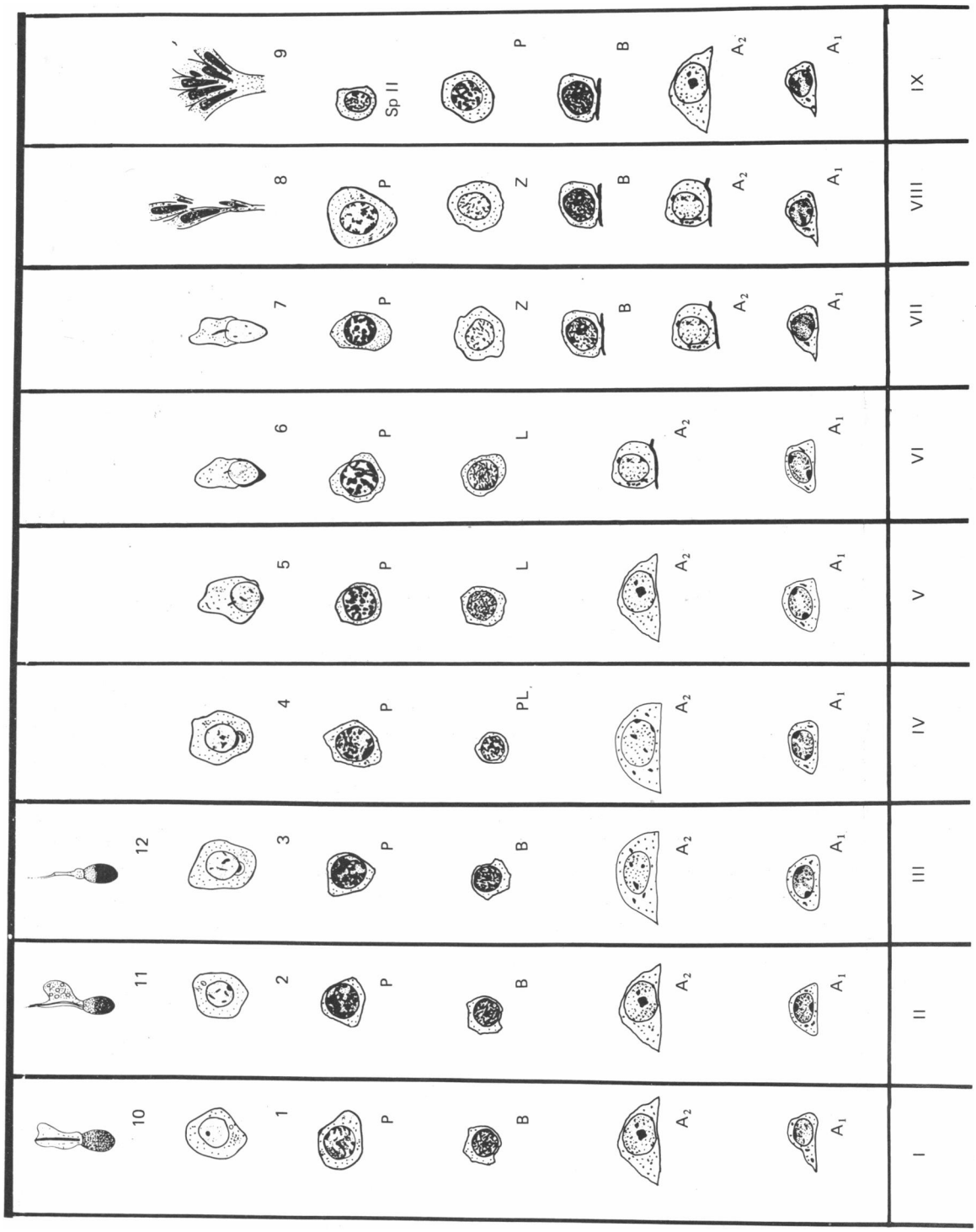
I
II
III
IV
V
VI
VII
VIII
IX
10
11
12
1
2
3
4
5
6
7
8
9
P
B
A1
A2
PL
L
Z
Sp II

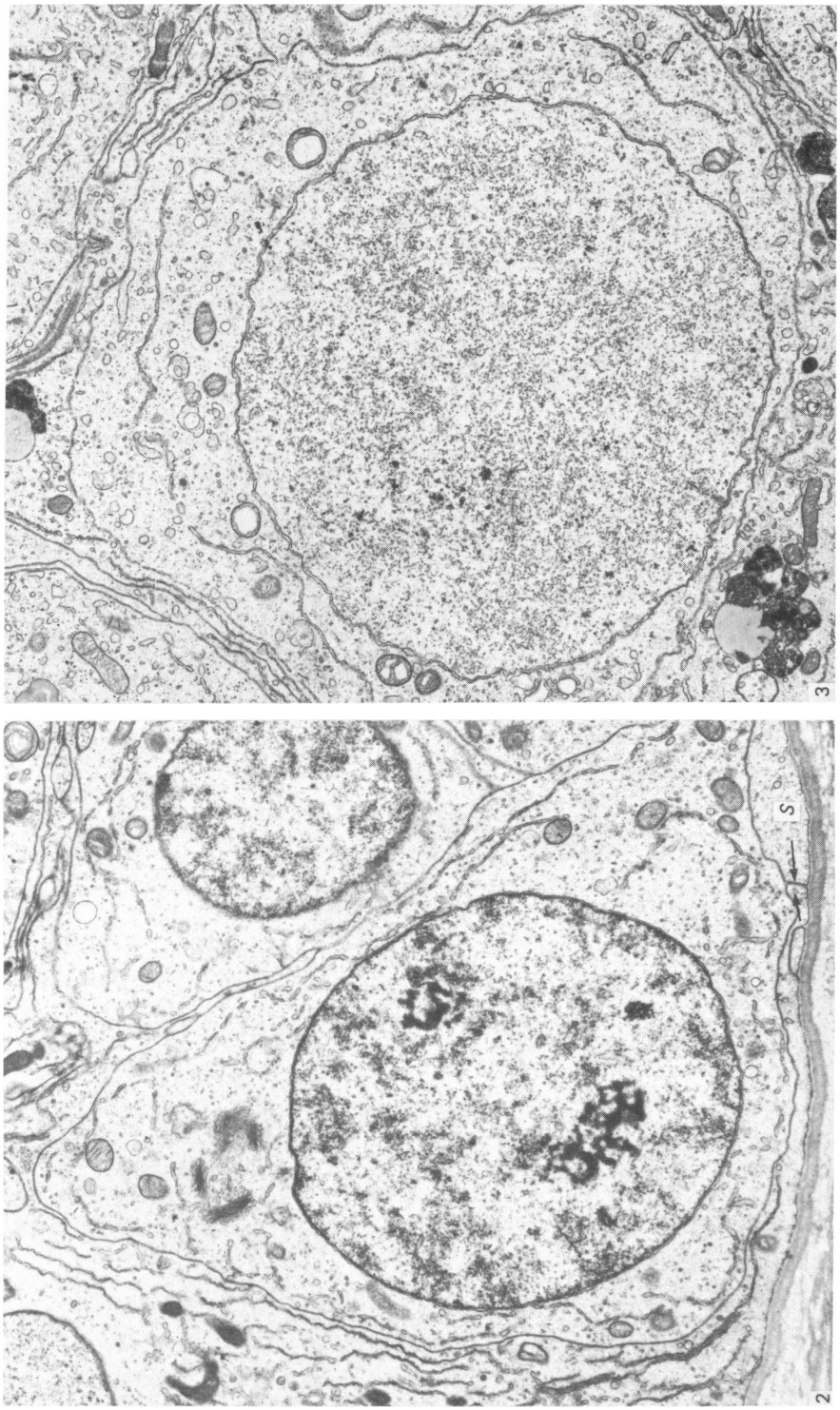

Fig. 2. A preleptotene spermatocyte is shown, separated from the basal lamina of the seminiferous epithelium by thin processes of Sertoli cell cytoplasm (*S*), extending inwards from both sides and forming a junction (arrows). The spherical nucleus contains coarse chromatin and two nucleolar regions. ×7500.

Fig. 3. This electron micrograph shows a primary spermatocyte in early zygotene. The mitochondria have developed a conspicuously swollen appearance, and the nucleoplasm is finely granular. ×9200.

The most obvious identifying feature of Stage IV was the presence of preleptotene spermatocytes. These cells were readily recognisable by their characteristically spherical nuclei, their small size in comparison with their precursors, the Type B spermatogonia, and by their distribution close to the basal lamina of the seminiferous tubule.

Stages V–VII of the spermatogenic cycle involved the remodelling of the (Steps 5–7) spermatids, together with the transition of the younger spermatocyte generation from the preleptotene stage of meiosis through leptotene (Stages V and VI) into zygotene primary spermatocytes (Stage VII). Stage VIII was identified by the first appearance of spermatid bundles within Sertoli cells, as well as the expanded appearance of the pachytene spermatocyte nuclei, as these cells approached division into secondary spermatocytes.

Three generations of spermatogonia were readily recognised by light microscopy, Types A_1, A_2 and B, corresponding to the descriptions given by Clermont (1969) for primates. Type A_2 cells were larger than Type A_1; their nuclei contained finely granular, lightly staining material and one or two well developed nucleoli. Type B spermatogonia were typically rounded cells containing coarse, darkly staining chromatin. More than one form of Type B spermatogonium was observed in the marmoset testis, but quantitative analyses were not performed to define the number of Type B spermatogonial divisions.

Electron microscopy

Spermatocyte development

Preleptotene spermatocytes (Fig. 2) were found in Stage IV of the spermatogenic cycle, situated near the basal lamina but separated from it by Sertoli cell processes. Typically, these spermatocytes were conical in shape, with a central, spherical nucleus. Their nuclei contained clumps of chromatin, preferentially associated with the nuclear membrane (Fig. 2); one or two well developed nucleoli were frequently observed.

The cytoplasm of preleptotene spermatocytes contained a few strands of endoplasmic reticulum, two or three stacks of Golgi lamellae arranged adjacent to one another (Fig. 2) and a number of small mitochondria. Small, circular profiles of membranous vesicles were also observed in the cytoplasm, as well as many small granules, probably free ribosomes. Cytoplasmic bridges frequently interconnected these cells and this feature persisted during the more advanced stages of spermatogenic differentiation.

The development of spermatocytes from the preleptotene to the leptotene and zygotene stages of meiosis involved an increase in cell size and a conspicuous change in nuclear structure. The chromatin aggregation which typified preleptotene spermatocytes gave way to a finely granular appearance within the nucleoplasm (Fig. 3). During the early zygotene stage, synaptonemal complexes became visible and endoplasmic reticulum became associated with the nuclear membrane. Subsequently the number of continuous lengths of endoplasmic reticulum lamellae overlying the nuclear membrane increased from one up to five or six (Fig. 4) during Stages I–V, followed later by separation from the nuclear membrane prior to the second meiotic division.

During spermatocyte development the mitochondria lost their compact appearance and became swollen, as if fluid-filled. This appearance was maintained throughout most of the spermiogenic sequence, only to be lost at about the time of middle-piece assembly in mature spermatids.

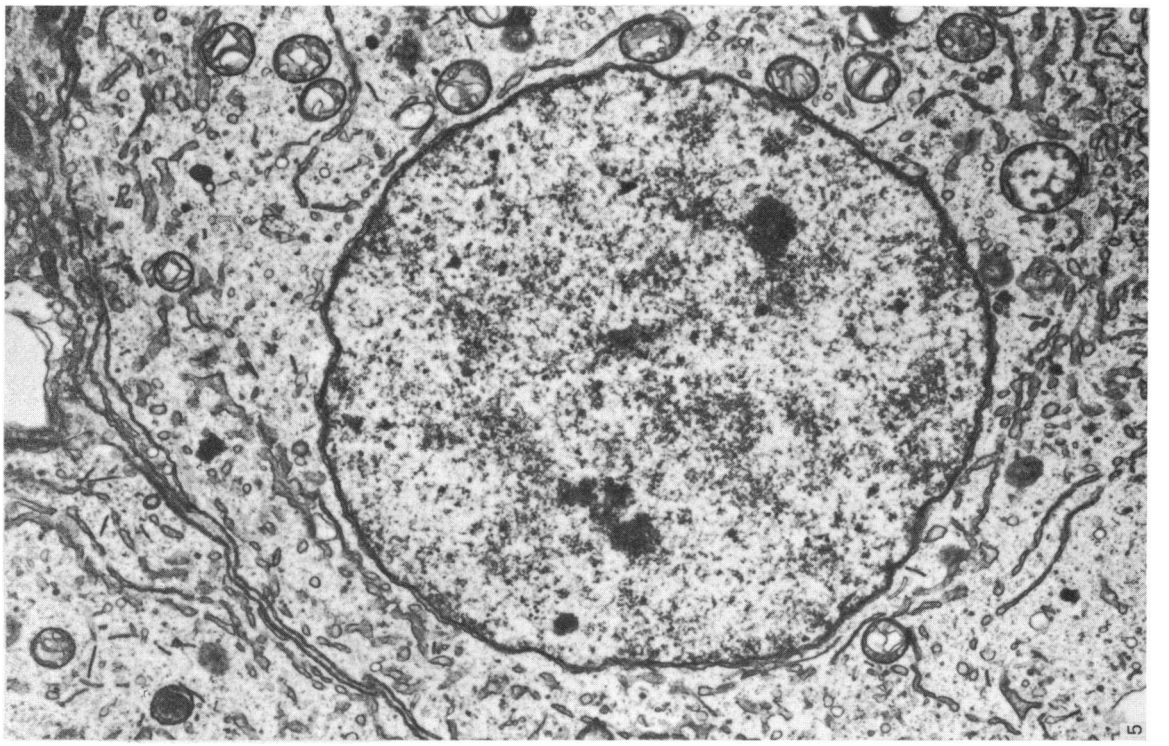

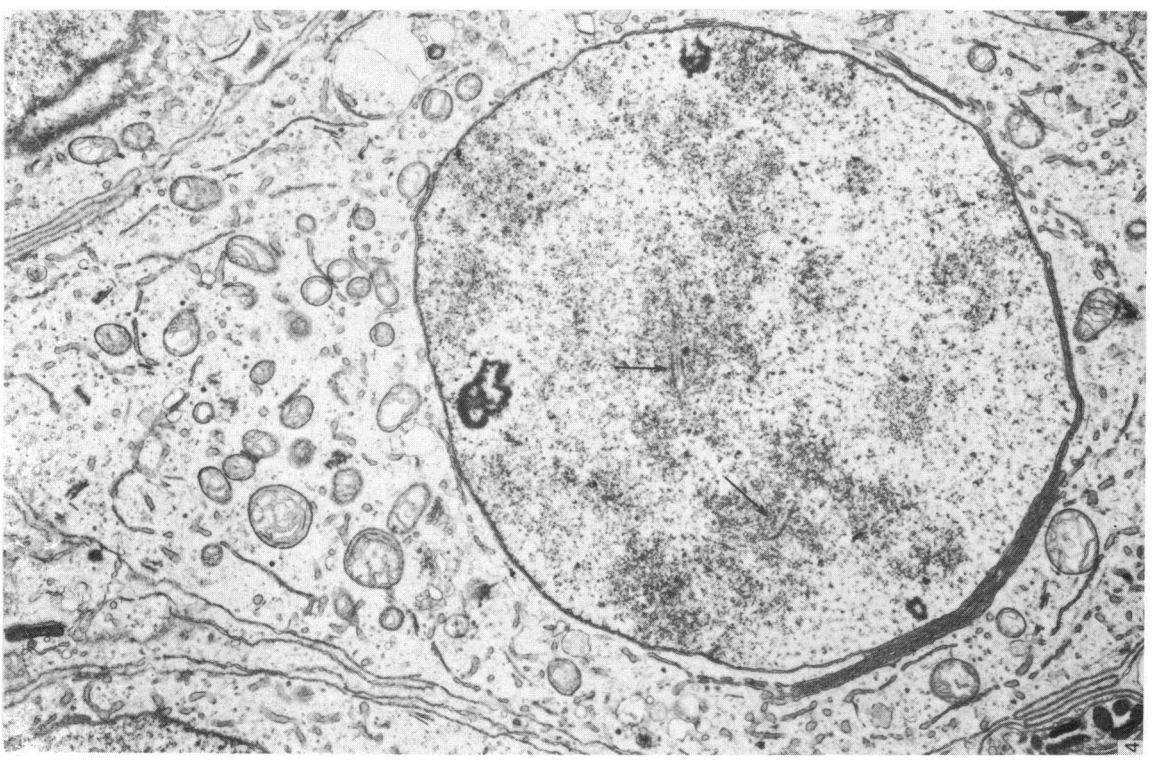

In addition to the cytoplasmic bridges which interconnected the spermatocytes, other types of intercellular junctions were also observed. A number of desmosomes joined the spermatocyte plasma membrane with that of neighbouring Sertoli cells, and late in the pachytene stage, at about Stage VII, there was development of Sertoli cell ectoplasmic (Russell, 1977) specialisations. These specialisations of the Sertoli cell plasma membrane were characterised by accumulations of actin filaments immediately beneath the cell surface.

Secondary spermatocytes were smaller than their precursor generation of primary spermatocytes and contained coarser heterochromatin (Fig. 5). Abundant endoplasmic reticulum was visible in the cytoplasm and localised concentrations of lamellae and vesicles were occasionally present.

Spermiogenesis

The developmental changes in spermatid structure during spermiogenesis were similar to those seen in other mammals, and were classified into twelve steps. The distinctions between steps were readily appreciated by electron microscopy although the steps were difficult to distinguish reliably by light microscopy.

The early phase of Step 1 was characterised by the presence of a proacrosomal vesicle situated near the highly developed Golgi apparatus (Fig. 6). In this phase, and later in Step 1, when the proacrosomal vesicle was enlarged and became applied to one pole of the nucleus (Fig. 7), the mitochondria tended to be clustered in the vicinity of the Golgi apparatus. Sertoli cell ectoplasmic specialisations, mentioned earlier in connection with pachytene spermatocytes, bordered part of the young spermatids and remained associated with all subsequent steps of spermiogenesis until breaking down shortly before spermiation.

Steps 2–4 of spermiogenesis (Figs. 8, 9) involved flattening of the proacrosomal vesicle against one pole of the spermatid nucleus, and synthesis of acrosomal contents, as judged by the presence of flocculent masses within the vesicle and the deposition of dense acrosomal material. During the early stages, the Golgi apparatus consisted of several lamellae arranged in a crescent with its concavity facing the acrosome (Fig. 8). Interposed between the Golgi lamellae and the outer acrosomal membrane were numerous membranous vesicles, mostly circular in profile, although short, narrow and straight profiles also occurred. Endoplasmic reticulum was present near the convex aspect of the Golgi apparatus, and numerous small vesicles were situated between these two organelles.

Between Steps 4 and 7 the spermatid nucleus became flattened, and some condensation of the chromatin granules occurred. The apical segment of the acrosome became extended anteriorly at about Step 7 (Fig. 11); prior to this event, in favourable planes (Fig. 10, arrowhead), a membranous whorl was observed in the subacrosomal space immediately beneath the apical segment.

Nuclear condensation continued between Steps 7 and 10, when it was virtually complete and the spermatid head had assumed its final shape (Fig. 13). The nuclear matrix contained a variable number of vacuoles at this stage and a considerable

Fig. 4. A pachytene spermatocyte in Stage IV of spermatogenesis is shown in this electron micrograph. One pole of the nucleus is bordered by a stack of endoplasmic reticulum lamellae, and a number of synaptonemal complexes are visible within the nucleoplasm (arrows). Mitochondria and strands of endoplasmic reticulum are scattered throughout the cytoplasm, frequently in close association with one another. × 12 500.

Fig. 5. A secondary spermatocyte is shown in this electron micrograph. The nucleus contains coarse chromatin, scattered throughout the nucleoplasm. × 12 500.

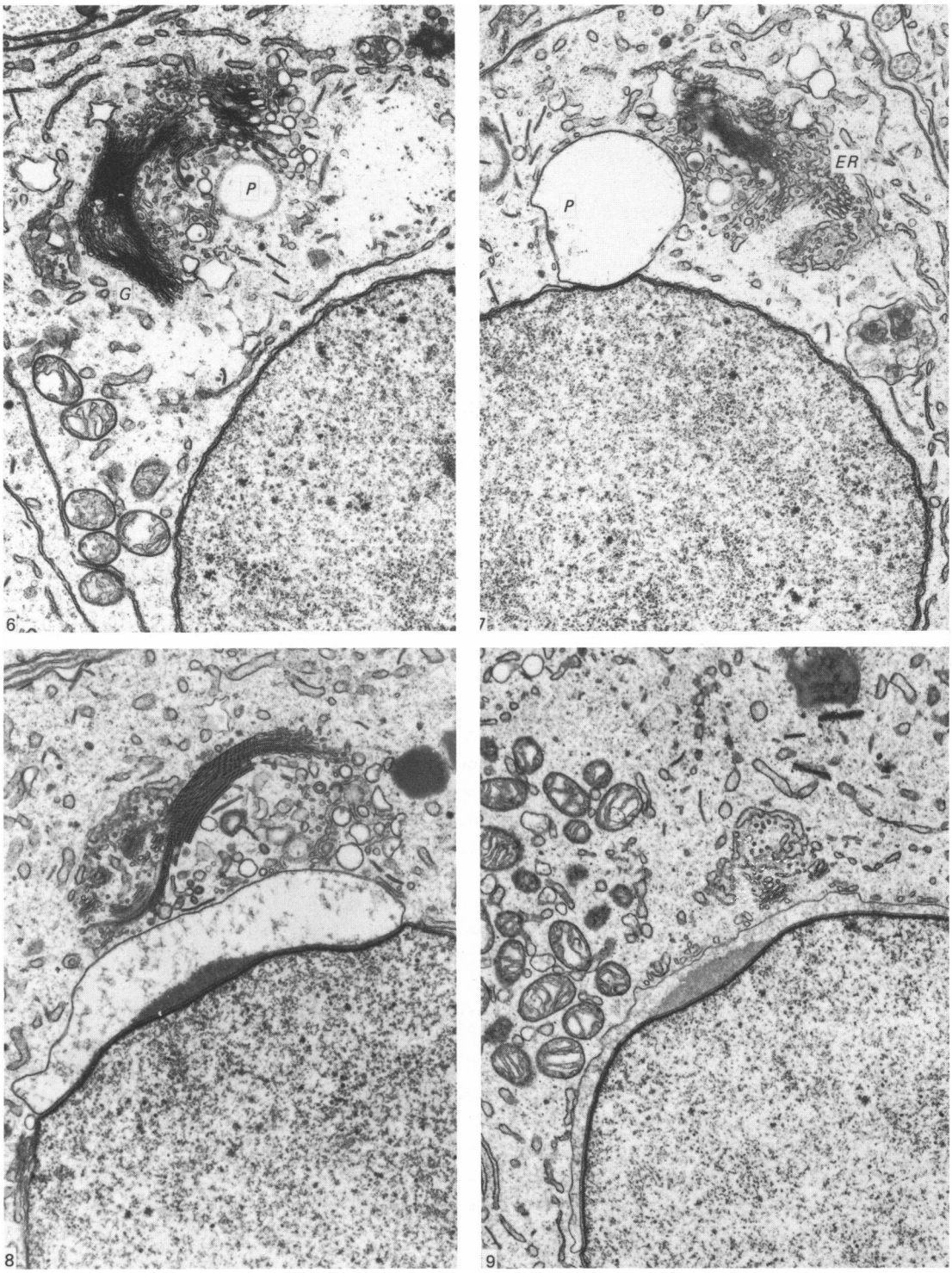

Figs. 6–9. These figures depict the early steps of spermiogenesis in the marmoset, commencing with the formation of a proacrosomal vacuole and its movement towards the nucleus (Figs. 6, 7). The formation of the proacrosomal granule (*P*) occurs in the vicinity of the highly developed Golgi apparatus (*G*) and numerous small vesicles. Extensive development of the endoplasmic reticulum (*ER*) adjacent to the Golgi apparatus, is a conspicuous feature in Fig. 7. Figs. 8 and 9 show acrosomal development in Steps 3 and 4 respectively, when the proacrosomal vacuole becomes flattened over one pole of the nucleus. A cluster of mitochondria is evident adjacent to the developing acrosome in Fig. 9. × 12500.

amount of redundant nuclear membrane was formed (Fig. 12, *RNM*). By Step 9, however, the annulus had not commenced its caudal migration and the mitochondria were not yet arranged helically about the axial filament. This process, and formation of the residual body, took place between Steps 10 and 11 (Fig. 15). Late in Step 11, spermiation occurred, preceded by the formation of tubulobulbar complexes (Fig. 14), and extensive invaginations of Sertoli cell plasma membrane which also involved uptake of the spermatid plasma membrane.

During the final development of the sperm tail in the marmoset, prior to the caudal migration of the annulus in Step 10/11, a swelling of the posterior middle-piece became apparent. It was filled with a regular lattice array, and its posterior boundary marked the zone between the future middle-piece and main-piece (Fig. 16). The fibrous sheath of the main-piece was itself somewhat irregular at this stage, being interspersed with a number of vacuoles (Fig. 16). These vacuoles, and the swelling noted above, disappeared before spermiation occurred.

Spermiation took place during Stage III of spermatogenesis, apparently coinciding with the last mitotic divisions of Type B spermatogonia, as judged by the observation of spermatogonial mitotic figures at this time.

DISCUSSION

The division of the spermatogenic cycle of the marmoset monkey into nine distinctive cell associations represents an attempt to produce a basic system for analytical and ultrastructural studies in this species. Whilst being sufficiently detailed to be useful, it is designed to minimise the possible mis-identification and confusion of spermatogenic stages.

Previous studies of the spermatogenic cycle in primates (Clermont, 1969; Chowdhury & Steinberger, 1976; Dym, 1977) have used classification systems involving twelve separate stages of spermatogenesis and fourteen steps of spermatid development. Careful consideration of the present observations, however, has led to the view that only nine stages of spermatogenesis, with twelve spermiogenic steps, can be identified unequivocally in the marmoset.

The system of nine stages used here relies less than do the earlier systems upon the recognition of subtle morphological differences in acrosomal structure as a key to stage identification. Instead, the association of cell types in any particular region of the seminiferous epithelium is used to define the spermatogenic stage. This method has a distinct advantage when applied to the marmoset, since the acrosome in this species is small and unobtrusive.

Classification of the spermatogenic cycle in this way does not represent a new departure from established procedures. For example, similar systems have been applied in studies of bull (Berndtson & Desjardins, 1974), stallion (Swierstra, Gebauer & Pickett, 1974) and African elephant (Johnson & Buss, 1967) spermatogenesis. Classical histologists such as Benda, Von Ebner and Regaud also developed such systems for studying the spermatogenic wave (for review see Curtis, 1918).

The main differences between the twelve stage systems used by previous investigators and the nine stage classification used here lie in the early stages of spermatogenesis, i.e. Stages I–V. Clermont's (1969) system, later used by Dym & Cavicchia (1977), distinguished Stages I–V on the basis of changing spermatid morphology, with the recognition of five early steps of spermiogenesis, and on the differentiation of Type B spermatogonia, of which four generations were noted. As no quantitative


RNM
12

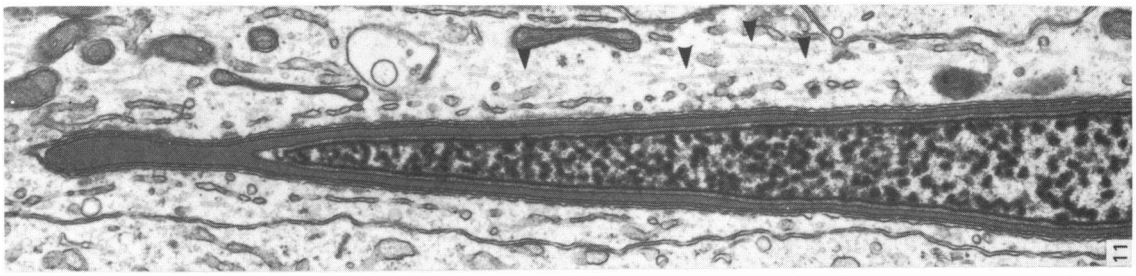
11

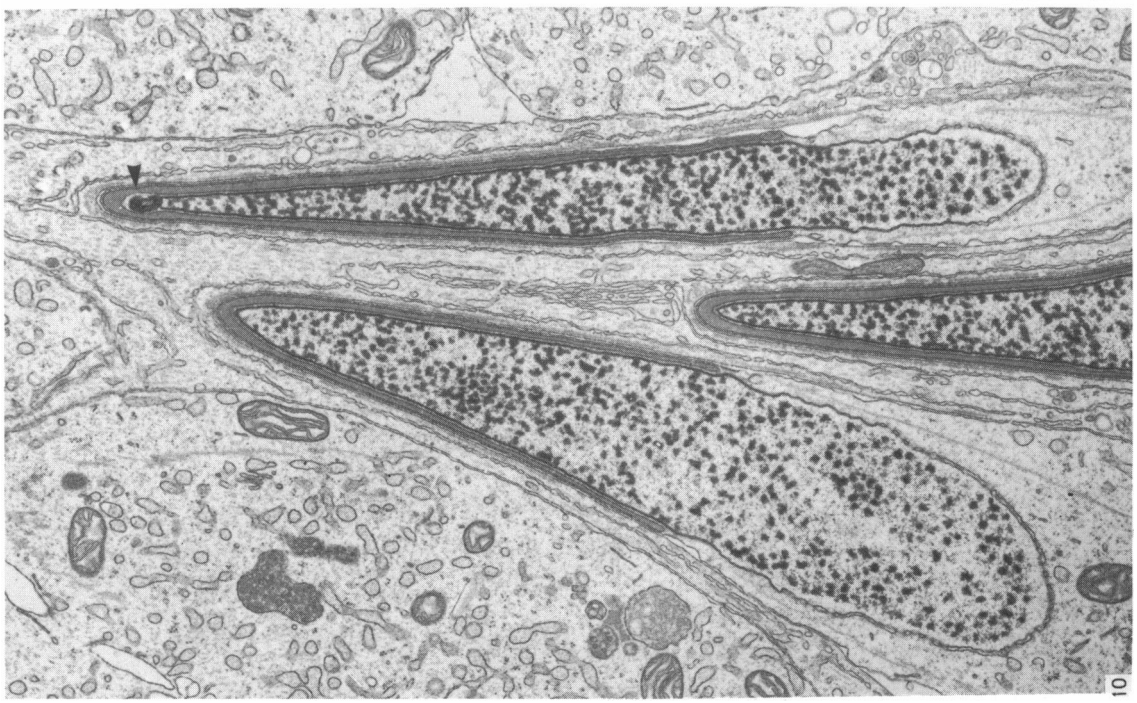
10

analyses of spermatogonial divisions were performed in the present study, the various generations of Type B spermatogonia could not be distinguished unequivocally, although several variations in nuclear structure have been observed in these cells.

In addition, the differences between acrosomal structure in spermatids at Steps 1–4 in Clermont's system have been judged to be too fine for reliable distinctions to be made. Thus, Clermont's Stages I–V have been condensed into Stages I–III of the present system. Stages IV–IX of the present system correspond exactly to Clermont's Stages VII–XII.

The ultrastructure of marmoset spermatocytes, from the preleptotene to the secondary spermatocyte stages of differentiation, closely resembles that described by Dym & Cavicchia (1978) in other monkeys. One notable feature of spermatocyte differentiation is the elaboration of the endoplasmic reticulum, and especially its close association with the nuclear membrane. Similar observations have been made by Dym & Cavicchia (1978) in monkeys, but in a more detailed examination of this phenomenon in the human spermatocyte, Nistal, Paniagua & Esponda (1980) suggest that the endoplasmic reticulum is actually derived from the nuclear membrane. The observations presented here tend to favour this proposal, although cytochemical studies are probably required to prove it.

Despite this similarity with the human spermatocyte, a special formation of the endoplasmic reticulum, the 'annulate lamellae', has not been observed in the marmoset. This formation is said to be characteristic of human spermatocytes and spermatids (Smith & Berlin, 1977; Nistal *et al.* 1980), but is not reported by Dym & Cavicchia (1978) in their ultrastructural study of spermatogenesis in monkeys.

The early stages of spermiogenesis in the marmoset correspond closely to the pattern seen in other mammalian species, where the acrosomal vesicle is formed by the coalescence of smaller vesicles, then approaches and flattens itself over one pole of the spermatid nucleus. At this stage, synthesis of both acrosomal membrane and acrosomal contents probably takes place within the Golgi apparatus. This is indicated by the numerous membranous vesicles interposed between these two organelles, and by the loosely flocculent material lying within the acrosome, which eventually condenses into a compact granule.

The presence of ribosomes on the acrosomal membrane itself has been reported in the guinea-pig (Mollenhauer & Morré, 1978), suggesting that direct transmembrane protein synthesis of acrosomal proteins may occur. Although this was specifically investigated in the marmoset, no such association has been found.

The later stages of flagellar development in the marmoset spermatid involve the formation and disappearance of a bulbous complex of regularly distributed fibres in paracrystalline array, which surrounds the developing axoneme prior to the caudal migration of the annulus. Similar structures have been observed in man (Wartenberg & Holstein, 1975), the cottontop tamarin (Rattner & Brinkley, 1970) and non-primate species (Pedersen, 1969) where they have been termed the spindle-shaped body or tubular complex.

Figs. 10–12. These figures show some later stages of spermiogenesis between Steps 6 and 8. Figure 10 shows spermatids at Step 6/7 of spermiogenesis, when they are aligned by the Sertoli cells into centrifugally directed groups. At this stage and thereafter the Sertoli cell cytoplasm adjacent to the spermatids contains numerous, parallel microtubules arranged longitudinally (Figs. 11, 12, arrowheads). One spermatid shown in Figure 10 possesses a membranous whorl lying immediately above the anterior margin of the nucleus (arrowhead). A notable feature of the spermatid in Figure 12 is the considerable amount of redundant nuclear membrane (*RNM*) situated at the posterior end of the nucleus. (10) × 12500; (11, 12) × 18750.

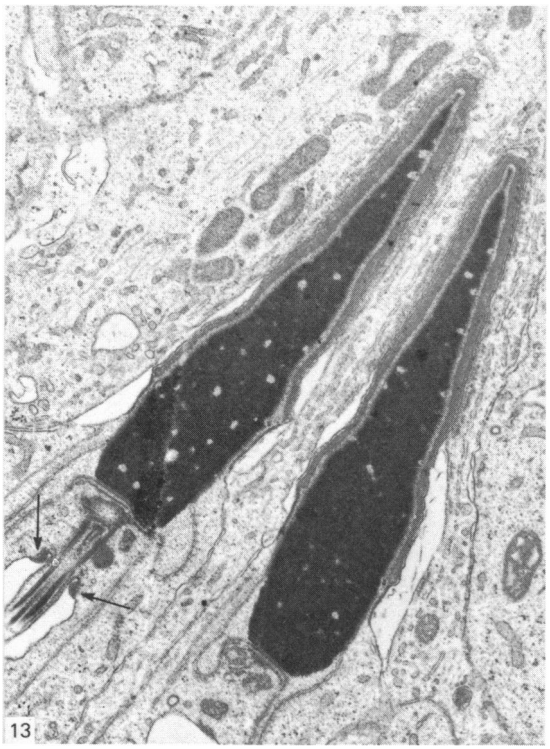

13

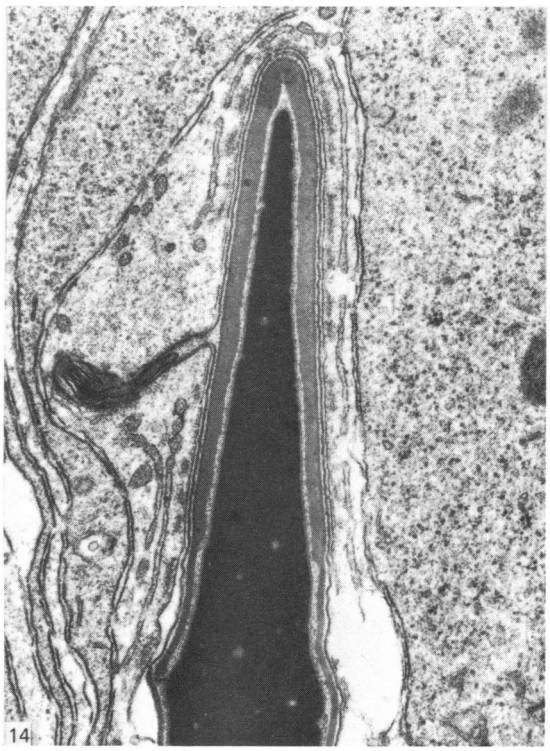

14

15

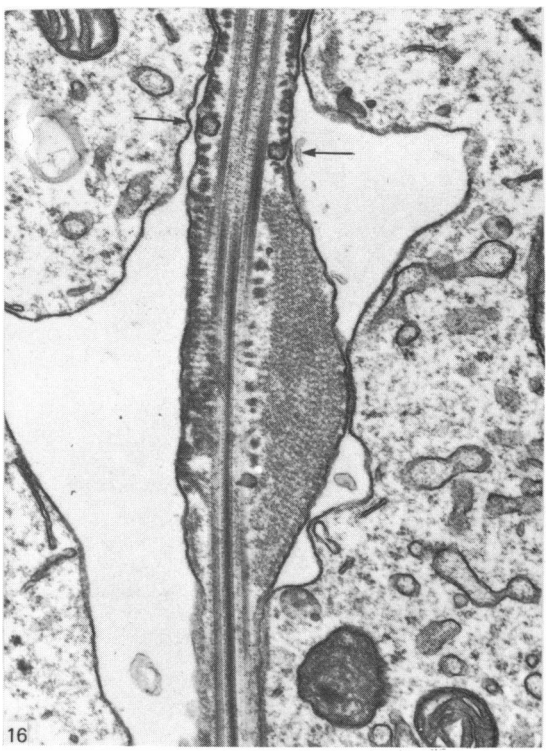

16

The development of tubulobulbar complexes late in spermiogenesis is a phenomenon of considerable interest, since it may have important implications for the biogenesis and differentiation of the sperm plasma membrane. Such structures, involved in uptake and removal by Sertoli cells of the spermatid plasma membrane, have been observed in a range of species (Russell & Clermont, 1976; Russell, 1979*a*, *b*) and are thought to function in the shedding of excess cytoplasm. However, as it appears that spermatid head membranes, i.e. the nuclear membrane and acrosomal membrane, are initially produced in excess and are lost by various mechanisms (Franklin, 1968; Courtens, 1978), the tubulobulbar complex may be a similar device for the elimination of excess plasma membrane. It would be of considerable interest to discover whether membrane components are preferentially removed by tubulobulbar complexes.

SUMMARY

The pattern of normal spermatogenesis in the common marmoset, *Callithrix jacchus*, is described and a system classifying the spermatogenic cycle into nine successive stages is presented. In contrast to most previous studies of spermatogenesis, the classification system developed in this study depends more upon the recognition of characteristic cell associations rather than upon identification of particular steps of spermatid development. The structurally simple acrosome of the marmoset spermatozoon displays insufficiently clear morphological changes during spermatid elongation to allow this to be used as a key to spermatogenic classification.

Ultrastructural aspects of spermatogenesis in the marmoset are also described; in general, these correspond to similar descriptions of this process in other primates.

We would like to thank Dr R. Siddall (ICI Ltd) who kindly provided the animals used in this study. This investigation was supported by a grant from the Medical Research Council.

Fig. 13. The spermatids shown in this Figure are at Step 9 of spermiogenesis. The annulus (arrows) has not yet migrated posteriorly, and formation of the middle-piece is therefore incomplete. The spermatid heads have, however, assumed their final shape, and nuclear condensation is complete. × 12500.

Fig. 14. This Figure shows a spermatid in Step 11 of spermiogenesis, a tubulobulbar complex being present adjacent to the principal segment of the acrosome. This structure is formed from an extrusion of the spermatid plasma membrane into an invagination of the Sertoli cell plasma membrane. Membrane whorls are present within the tubulobulbar complex. × 25000.

Fig. 15. This Figure shows a longitudinal section through the middle-piece and residual body (*RB*) of a spermatid in Step 11 of spermiogenesis. Annular migration has been completed and the mitochondria are situated around the flagellum. The residual body contains several densely stained spherical bodies, and is connected to an adjacent spermatid by a cytoplasmic bridge (arrowhead). × 12500.

Fig. 16. This micrograph shows a portion of the middle-piece of a Step 9 spermatid prior to caudal migration of the annulus. Circular membrane profiles are situated within the axonemal complex of the main piece (arrows) and a large array of paracrystalline material forms a swelling at the boundary between the middle-piece and main-piece. In this Figure, the more posterior regions of the sperm tail are situated uppermost. × 25000.

REFERENCES

ANTAR, M. (1971). Duration of the cycle of the seminiferous epithelium and of spermatogenesis in the monkey (*Macaca speciosa*). *Anatomical Record* **169**, 268–269.

BARR, A. B. (1973). Timing of spermatogenesis in four non human primate species. *Fertility and Sterility* **24**, 381–389.

BERNDTSON, W. E. & DESJARDINS, C. (1974). The cycle of the seminiferous epithelium and spermatogenesis in the bovine testis. *American Journal of Anatomy* **140**, 167–180.

CAVICCHIA, J. C. & DYM, M. (1978). Ultrastructural characteristics of monkey spermatogonia and preleptotene spermatocytes. *Biology of Reproduction* **18**, 219–228.

CHOWDHURY, A. K. & STEINBERGER, E. (1976). A study of germ cell morphology and duration of spermatogenic cycle in the baboon, *Papio anubis*. *Anatomical Record* **185**, 155–170.

CLERMONT, Y. (1969). Two classes of spermatogonial stem cells in the monkey (*Cercopithecus aethiops*). *American Journal of Anatomy* **126**, 57–72.

CLERMONT, Y. & LEBLOND, C. P. (1959). Differentiation and renewal of spermatogonia in the monkey, *Macaca rhesus*. *American Journal of Anatomy* **104**, 237–273.

CLERMONT, Y. & ANTAR, M. (1973). Duration of the cycle of the seminiferous epithelium and the spermatogonial renewal in the monkey *Macaca arctoides*. *American Journal of Anatomy* **136**, 153–166.

COURTENS, J. L. (1978). Release of carbohydrate-containing vesicles by the developing acrosomes of ram spermatids – relation to morphometric changes of the acrosome. *Journal of Ultrastructure Research* **65**, 182–189.

CURTIS, G. M. (1918). The morphology of the mammalian seminiferous tubule. *American Journal of Anatomy* **24**, 339–394.

DYM, M. (1973). The fine structure of the monkey (*Macaca*) Sertoli cell and its role in maintaining the blood–testis barrier. *Anatomical Record* **175**, 639–656.

DYM, M. (1977). The male reproductive system. In *Histology* (ed. L. Weiss & R. O. Greep), pp. 979–1038. New York: McGraw-Hill.

DYM, M. & CAVICCHIA, J. C. (1977). Further observations on the blood–testis barrier in monkeys. *Biology of Reproduction* **17**, 390–403.

DYM, M. & CAVICCHIA, J. C. (1978). Functional morphology of the testis. *Biology of Reproduction* **18**, 1–15.

FRANKLIN, L. E. (1968). Formation of the redundant nuclear envelope in monkey spermatids. *Anatomical Record* **161**, 149–162.

JOHNSON, O. W. & BUSS, I. O. (1967). The testes of the African elephant (*Loxodonta africana*). *Journal of Reproduction and Fertility* **13**, 11–21.

LILLIE, R. D. & FULLMER, H. M. (1976). *Histopathologic Technic and Practical Histochemistry*, 4th ed. New York: McGraw-Hill.

MOLLENHAUER, H. H. & MORRÉ, D. J. (1978). Polyribosomes associated with forming acrosome membranes in guinea pig spermatids. *Science* **200**, 85–86.

NISTAL, M., PANIAGUA, R. & ESPONDA, P. (1980). Development of the endoplasmic reticulum during human spermatogenesis. *Acta anatomica* **108**, 238–249.

PEDERSEN, H. (1969). Microtubules in the spermatid of the rabbit. *Zeitschrift für Zellforschung und mikroskopische Anatomie* **98**, 148–156.

RATTNER, J. B. & BRINKLEY, B. R. (1970). Ultrastructure of mammalian spermiogenesis. 1. A tubular complex in developing sperm of the cottontop marmoset *Sequinus oedipus*. *Journal of Ultrastructure Research* **32**, 316–322.

RUSSELL, L. (1977). Observations on rat Sertoli ectoplasmic ('*junctional*') specializations in their association with germ cells of the rat testis. *Tissue and Cell* **9**, 475–498.

RUSSELL, L. D. (1979*a*). Further observations on tubulobulbar complexes formed by late spermatids and Sertoli cells in the rat testis. *Anatomical Record* **194**, 213–232.

RUSSELL, L. D. (1979*b*). Spermatid–Sertoli tubulobulbar complexes as devices for elimination of cytoplasm from the head region of late spermatids of the rat. *Anatomical Record* **194**, 233–246.

RUSSELL, L. & CLERMONT, Y. (1976). Anchoring devices between Sertoli cells and late spermatids in rat seminiferous tubules. *Anatomical Record* **185**, 259–278.

SMITH, F. E. & BERLIN, J. D. (1977). Cytoplasmic annulate lamellae in human spermatogenesis. *Cell and Tissue Research* **176**, 235–242.

SWIERSTRA, E. E., GEBAUER, M. R. & PICKETT, B. W. (1974). Reproductive physiology of the stallion. 1. Spermatogenesis and testis composition. *Journal of Reproduction and Fertility* **40**, 113–123.

VENABLE, J. H. & COGGESHALL, R. (1965). A simplified lead citrate stain for use in electron microscopy. *Journal of Cell Biology* **25**, 407–408.

WARTENBERG, H. & HOLSTEIN, A. F. (1975). Morphology of the 'spindle-shaped body' in the developing tail of human spermatids. *Cell and Tissue Research* **159**, 435–443.